2021 43rd Annual International Conference of the
IEEE Engineering in Medicine & Biology Society (EMBC)
Oct 31 - Nov 4, 2021. Virtual Conference

Contraction model of skeletal muscle driven by external electrical stimulation—Proposal and Identification— *

W. Hijikata, *Member, IEEE*, T. Mochida, *Student Member, IEEE*, J. Liu and W. Sugimoto

***Abstract*— Biohybrid actuators consisting of skeletal muscle and artificial lattice have unique characteristics such as self-growth and self-repair functions. As a first step for developing model-based design and model-based control methods for the biohybrid actuators, we have developed a muscle contraction model. When the stimulation voltage is applied to the muscle, the electrical charges are stored in the dihydropyridine receptor, and the calcium ions are released. According to the concentration of the ions, the contractile elements generate contraction force. We have modeled this phenomenon with three characteristics in the proposed model—electrical dynamic, physiological, and mechanical dynamic characteristics. Unlike the previous models, the proposed model was verified under the condition of tetanus and incomplete tetanus with the muscle length changed. The simulated contraction force showed good agreement with the experimentally measured contraction force generated by the gastrocnemius muscle of a toad.**

***Clinical Relevance*— Biohybrid actuators are expected as a new material for medical and assistive devices having a soft and flexible characteristic. This study provides a basic contraction model for such biohybrid actuators.**

I. Introduction

Many types of actuators—electromagnetic actuators, hydraulic actuators, piezoelectric actuators, and ultrasonic actuators—have been successfully put into practical use in the industrial and medical fields. Especially soft actuators are expected to shift the paradigm in the soft robots collaborating with people and in the wearable devices such as power assist suits[1]. Biohybrid actuators, which consist of skeletal muscle and artificial lattice, are considered as another future option for a drive source in soft robots. In addition to stretchable and flexible features shown in soft actuators, biohybrid actuators have the potential to provide unique functions such as self-growth and self-repair. Since the 2010s, many types of research around biohybrid actuators have been reported [2]. As a future application, not only the actuators driven by glucose but also muscle generators for the implantable medical devices have been studied [3][4]. The current trend in this field is to investigate the method for culturing the muscle tissue and assembling it with the artificial lattice. When we look ahead to future industrial applications, it is desirable to establish the model-based design and model-based control methods of the actuator to meet the required performance and control the contraction precisely. In order to achieve them, the relationship between the input and output in the muscle should be modeled.

Although the energy source of the actuator is glucose, the control input is square wave voltage in general. It is, hence, beneficial to establish a dynamic model of the biohybrid actuator—the input and output are stimulation voltage and contraction force, respectively—for appropriate design and precise control. The group of Rockenfeller has established a detailed muscle contraction model based on a well-known Hill-type model [5]. The contraction forces calculated from the model and experimentally measured showed good agreement with each other. The model is, however, rather complex and verified only with the tetanic contraction under the isometric condition.

In this study, we divide the whole contraction process into three dynamics—electrical, physiological, and mechanical—. In the proposed model, those three dynamics are connected in series. The accuracy of the model was verified with the actual gastrocnemius muscle of toads.

II. Proposed Muscle Contraction Model

A. Overview

When the stimulation voltage v is applied to the skeletal muscle, calcium ions in the sarcoplasmic reticulum are released through Ryanodine receptors (RyR) according to the electrical charges q_c stored in the dihydropyridine receptor (DHPR). Based on the concentration of the calcium ions [Ca^{2+}], contractile elements consisting of actin and myosin

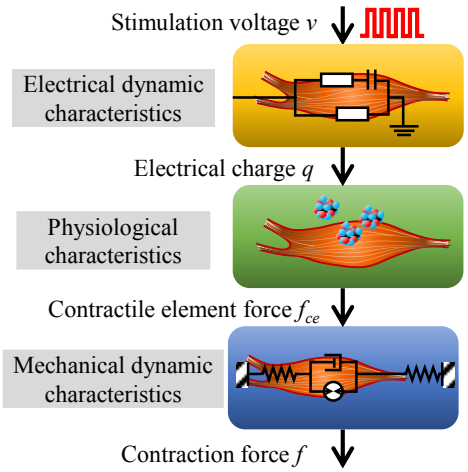

Figure 1. Overview of the proposed muscle contraction model. The model is divided into three parts; Electrical dynamic characteristics, Physiological characteristics, and Mechanical dynamic characteristics. The input is stimulation voltage and the output is the contraction force.

*Research supported by Japan Society for the Promotion of Science, Grant/Award Number 18K18830.

W. Hijikata, T. Mochida, J. Liu and W. Sugimoto are with the Tokyo Institute of Technology, Ookayama, Meguro-ku, Tokyo, 1528550, Japan (corresponding author to provide phone/fax +81-3-5734-2200; Email: hijikata.w.aa@m.titech.ac.jp)

generate internal contraction force f_{ce}. The entire muscle is a collection of the contractile elements and has elastic and viscous characteristics. As a result of internal interactions of these characteristics, contraction force f appears externally.

We have modeled the above mechanism such that the electrical dynamic, physiological and mechanical dynamic characteristics are connected in series as shown in Fig. 1. The dynamics are described in detail in the following.

B. Electrical dynamic characteristics

When the voltage is applied to the muscle, the electrical charge is stored in the DHPR. We modeled this reaction with the equivalent electrical circuit as shown in Fig. 2. R_{in} and R_{ex} represent the resistance of intracellular fluid and that of extracellular fluid, respectively. C is the capacity of the cell membrane. Note that the charge stored in C is regarded as DHPR charge q_c and is calculated as

$$v = R_{in} i_{in} + \frac{1}{C} \int i_{in} dt \tag{1}$$

$$q_c = \left| \int i_{in} dt \right|. \tag{2}$$

Where i_{in} is the current flown in C.

C. Physiological characteristics

There is a time delay between the supply of charges and the generation of contraction force. To express this, we consider a dead time t_0, as

$$q_c'(t) = q_c(t - t_0). \tag{3}$$

When the DHPR charge exceeds thresholds q_{th}, calcium ions are released from RyR [6]. We simply assumed the rate of the ion release $d[\mathrm{Ca}^{2+}]/dt$ is proportional to the DHPR charges as follows

$$\frac{d[\mathrm{Ca}^{2+}]}{dt} = a_{c1}(q_c' - q_{th})\zeta_q \tag{4}$$

$$\zeta_q = \frac{1}{1 + \exp[-10^{11}(q_c' - q_{th})]}. \tag{5}$$

a_{c1} is the proportional constant. ζ_q is the sigmoid function that changes from 0 to 1 as q_c' exceeds q_{th}. Note that the exponent value o10^{11} can be any value that is large enough.

At the same time, the calcium ions are recovered at a rate proportional to $[\mathrm{Ca}^{2+}]$ by the ion pumps [7]. We modeled these release and recovery of ions with the following convolutional integral

$$[\mathrm{Ca}^{2+}] = \int_0^t \frac{d[Ca^{2+}]}{dt'} \exp[-a_{c2}(t - t')]\, dt'. \tag{6}$$

a_{c2} is the constant that determines the recovery rate. In the actual calculation, we approximated (6) to the following discrete equation

$$[\mathrm{Ca}^{2+}]_n = \left. \frac{d[\mathrm{Ca}^{2+}]}{dt'} \right|_n \Delta t + \alpha^{\Delta t} [Ca^{2+}]_{n-1}. \tag{7}$$

Δt is the time step and a is the forgetting factor.

It is known that the contractile element force f_{ce} is increased with $[\mathrm{Ca}^{2+}]$ when it exceeds the threshold $[\mathrm{Ca}^{2+}]_{th}$ and

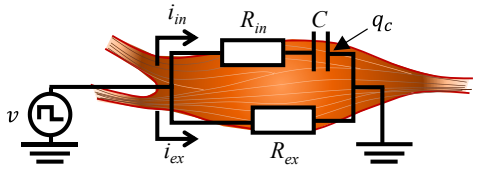

Figure 2. The equivalent electrical circuit of the electrical dynamic characteristics. The circuit is divided into two paths; one passes through intracellular fluid and the other passes through the extracellular fluid.

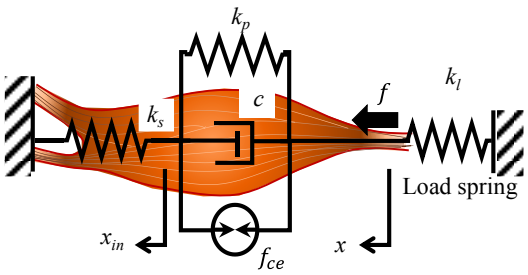

Figure 3. Model of the mechanical dynamic characteristics. The load spring can be changed according to the actual situation.

asymptotes to a maximum value f_{max} [8]. We described this relationship as

$$f_{ce} = f_{max}\{1 - \exp[-a_{c2}([Ca^{2+}] - [Ca^{2+}]_{th})]\}\zeta_{Ca}\ . \tag{8}$$

a_{c2} is the constant and ζ_{Ca} is the sigmoid function which is described as follow

$$\zeta_{\mathrm{Ca}} = \frac{1}{1 + \exp[-10^2([Ca^{2+}] - [Ca^{2+}]_{th})]}. \tag{9}$$

D. Mechanical dynamic characteristics

The contraction force of the muscle appears as a result of the interaction of viscoelastic properties of tissues and contractile element force. Several models have been proposed for this characteristic. In this study, we adopted the model shown in Fig. 3 as the mechanical dynamic characteristics. Note that this model assumed an external spring is connected to the muscle for a brief explanation. This spring can be changed depending on the type of the external load.

It is known that the elastic element k_s connected in series to the contractile element force is increased according to the muscle activation level. Based on this, we modeled k_s as a linear function of the contractile force as

$$k_s = a_{ms} f_{ce} + k_{s0}. \tag{10}$$

a_{ms} is the proportional constant and k_{s0} is the constant. The elastic element k_p connected to the contractile element in parallel has a value when the muscle is stretched beyond its natural length as follows

$$k_p = k_{p0}\zeta_x \tag{11}$$

$$\zeta_x = \frac{1}{1 + \exp(-10^{11}x)}. \tag{12}$$

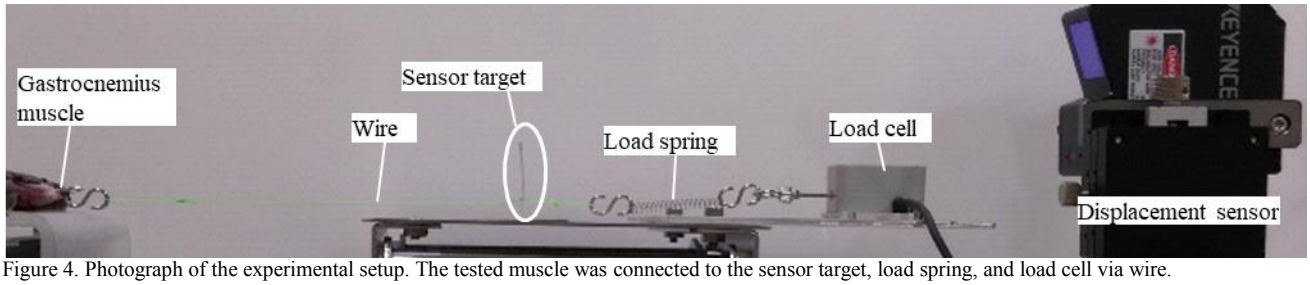

Figure 4. Photograph of the experimental setup. The tested muscle was connected to the sensor target, load spring, and load cell via wire.

k_{p0} is the constant, ζ_x is the sigmoid function and x is the contraction displacement. Note that the origin and positive direction of x are defined as natural length and contractile direction, respectively.

It is known that the viscosity and contraction velocity of the muscle has a relation of an exponential function; its maximum value is proportional to the contractile element force. Hence, we modeled the viscosity element c connected to the contractile element force as

$$c = a_{mc1} f_{ce} \exp(-a_{mc2}|\dot{x}|) + c_0. \quad (13)$$

a_{mc1} and a_{mc2} are the coefficients, x is the displacement of the entire muscle and c_0 is the constant.

From the balance of forces, the following equations can be derived.

$$c(\dot{x} - \dot{x}_{in}) = f_{ce} - f. \quad (14)$$

$$kx_{in} = -f. \quad (15)$$

$$f = k_l x. \quad (16)$$

x_{in} is the internal displacement of the muscle and k_l is the stiffness of the external spring. From (1)–(16), once the voltage is determined, the contraction force can be calculated.

III. Identification of the Model Parameters

A. Experimental Methods

The parameters in (1)-(16) are identified in experiments to verify the muscle contraction model. In the parameter identification, the gastrocnemius muscle in the hind leg of a readily available toad— Xenopus laevis—was used. Although approval for experiments with it was not required at Tokyo Institute of Technology, all the experiments were carried out in accordance with the guidelines for animal experimentation.

Fig. 4 shows the photograph of the measurement setup. A load spring with the stiffness of 100 N/m, a target for a laser displacement sensor (LK-G155, Keyence Co., Ltd., Osaka, Japan), and a load cell (LTS-1KA, Kyowa Electronic Instruments Co., Ltd, Tokyo, Japan) were connected to the calcaneal tendon of the toad in series via wire. Two needle-type stainless steel electrodes with diameters of 0.1 mm were run through the muscle.

Fig. 5 shows the schematic of the stimulation voltage. Pulse width and duration were fixed to 0.4 ms and 0.3 s. Two types of stimulations were applied to the muscle; one was to induce tetanus with an amplitude of 6.6 V and a cycle length of 0.0286 s (35 Hz); the other one was to induce incomplete tetanus with an amplitude of 4.2 V and a cycle length of 0.05 s (20 Hz).

Three parameters—R_{in}, C, and R_{ex}—in electrical dynamic characteristics were identified from the relationship between the stimulation voltage and current. The other parameters except for k_p were identified from the relationship between current and force. Since the muscle in this experiment only contracted and were always shorter than its natural length, the effect of k_p was not considered. The parameters are identified such that the sum of squire error between the experimental force and simulated force became minimum by using the sequential quadratic programming method.

The toad was anesthetized by immersing it in 0.1wt% tricaine water solution for 15 min. During the experiment, the anesthesia was maintained by wrapping the toad in a paper towel soaked with 0.05wt% tricaine water solution. After the experiments, the toad was electively killed. The experiment was carried out once within 12 hours.

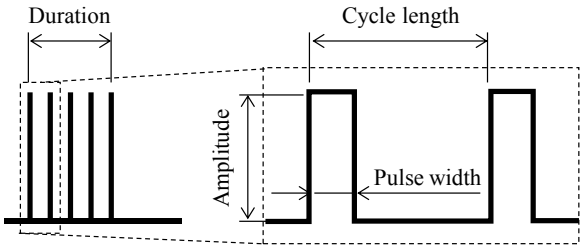

Figure 5. Schematic of the stimulation voltage. Pulse width and duration were fixed to 0.4 ms and 0.3 s. Amplitude and cycle length were changed so as to induce tetanus and incomplete tetanus.

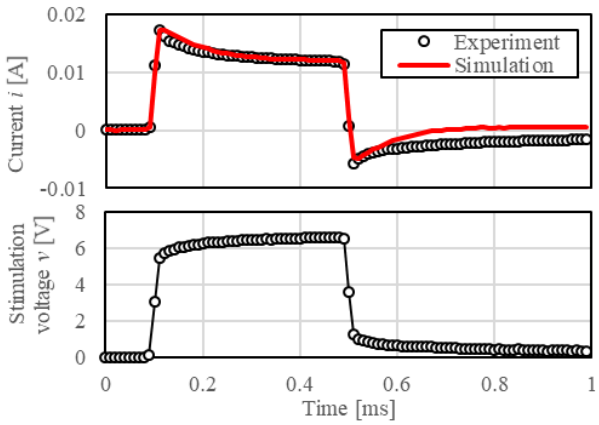

Figure 6. Measured current and simulated one with the identified parameters against the stimulation voltage with the amplitude of 6.6 V and pulse width of 0.4 ms. The simulated model of the electrical dynamic characteristics showed good agreement with the experimental results.

B. Result of parameter identification

Fig. 6 shows the measured current and simulated one with the identified parameters against the stimulation voltage with the amplitude of 6.6 V and pulse width of 0.4 ms. Although some errors were observed near the convergence of the current to zero, the peak value and the subsequent trend were generally consistent. By using these identified parameters, the other parameters were identified by using the force for tetanus and incomplete tetanus. Fig. 7 shows the comparison of the force measured in experiments and simulated in the model. The results showed good agreement with each other. TABLE I shows the identified parameters. Note that k_p is not considered in this research, it was treated as 0 in the simulation. The time

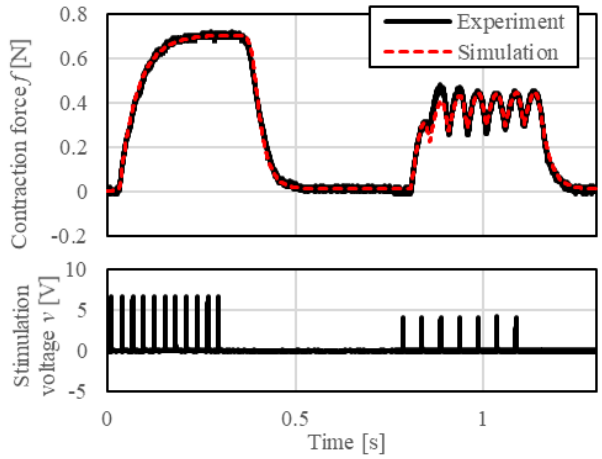

Figure 7. Measured contraction force and the simulated one. The former contraction is tetanus and the latter is incomplete tetanus. The model could express not only tetanus but also incomplete tetanus.

TABLE I. IDENTIFIED PARAMETERS

Identified parameters	Identified values	Unit
R_{in}	692	Ω
C	0.123×10^{-6}	F
R_{ex}	558	Ω
t_0	2.15×10^{-2}	s
q_{th}	0.412×10^{-6}	C
a_{c1}	4.00×10^{-10}	M/(s·C)
α	4.41×10^{-32}	-
Δt	1.00×10^{-5}	s
$[Ca^{2+}]_{th}$	3.03×10^{-2}	M
a_{c2}	13.6	-
f_{max}	0.704	N
k_{s0}	6.15×10^{6}	N/m
a_{ms}	3.00×10^{-9}	/m
k_{p0}	0 (not considered)	N/m
a_{mc1}	3.49	s/m
a_{mc2}	1.00×10^{-10}	-
c_0	2.37	N·s/m

the lag between the voltage and contraction force was identified by directly measuring it from the experimental data.

C. Discussion

The proposed model could express the contraction force well even under the condition with contraction displacement, incomplete tetanus, and twitch. This means the proposed model can be applied to control displacement and applications that use incomplete tetanus with high frequency, such as a flapping robot. This would be a great advantage of the proposed model over previous studies.

Some parameters such as a_{ms} and a_{mc2} became the lower limit in the parameter identification process. Hence k_s can be treated as constant and c can be treated as a simple linear function of f_{ce}. Although further investigation will be required, there is a possibility to simplify the contraction model through sensitivity analysis of parameters. This will be beneficial when we use the model to control the muscle contraction in biohybrid actuators in real time. We also plan to investigate how much the parameters will change in different muscles.

IV. CONCLUSION

We have proposed the muscle contraction model, which is divided into three parts; electrical dynamic, physiological, and mechanical dynamic characteristics. The model could simulate not only tetanus but also incomplete tetanus. Another outcome of this study is that the model could be applied even the muscle length changes during contraction. We plan to use this model for fast convergence calculations, which will be applied to the control and design of biohybrid actuators.

REFERENCES

[1] D. Rus and M. T. Tolley, "Design, fabrication and control of soft robots," *Nature*, vol. 521, no. 7553, pp. 467–475, May 2015.

[2] L. Ricotti *et al.*, "Biohybrid actuators for robotics: A review of devices actuated by living cells," *Sci. Robot.*, vol. 2, no. 12, pp. 1–18, 2017.

[3] G. Sahara, W. Hijikata, K. Tomioka, and T. Shinshi, "Implantable power generation system utilizing muscle contractions excited by electrical stimulation," *Proc. Inst. Mech. Eng. Part H J. Eng. Med.*, vol. 230, no. 6, pp. 569–578, 2016.

[4] T. Mochida and W. Hijikata, "Development of an energy harvesting device with a contactless plucking mechanism driven by a skeletal muscle," *J. Adv. Mech. Des. Syst. Manuf.*, vol. 13, no. 3, pp. 1–15, 2019.

[5] R. Rockenfeller *et al.*, "Exhaustion of Skeletal Muscle Fibers Within Seconds: Incorporating Phosphate Kinetics Into a Hill-Type Model," *Front. Physiol.*, vol. 11, no. May, 2020.

[6] W. Melzer, M. F. Schneider, B. J. Simon, and G. Szucs, "Intramembrane charge movement and calcium release in frog skeletal muscle.," *J. Physiol.*, vol. 373, no. 1, pp. 481–511, 1986.

[7] M. ENDO, "Conditions Required for Calcium-Induced Release of Calcium from the Sarcoplasmic Reticulum," *Proc. Jpn. Acad.*, vol. 51, no. 6, pp. 467–472, 1975.

[8] M. ENDO, "Stretch-induced Increase in Activation of Skinned Muscle Fibres by Calcium," *Nat. New Biol.*, vol. 237, no. 76, pp. 211–213, Jun. 1972.